Atmos. Chem. Phys. Discuss., https://doi.org/10.5194/acp-2017-1068
Manuscript under review for journal Atmos. Chem. Phys.
Discussion started: 21 November 2017

Atmospheric Chemistry and Physics Discussions

Reactive oxygen species (ROS) emissions and formation pathways in residential wood smoke under different combustion and aging conditions

Jun Zhou[1], Peter Zotter[2], Emily A. Bruns[1], Giulia Stefenelli[1], Deepika Bhattu[1], Samuel Brown[1,3], Amelie Bertrand[4], Nicolas Marchand[4], Houssni Lamkaddam[1], Jay G. Slowik[1], André S.H Prévôt[1], Urs Baltensperger[1], Thomas Nussbaumer[2], Imad El Haddad[1], and Josef Dommen[1]

[1]Laboratory of Atmospheric Chemistry, Paul Scherrer Institute, 5232 Villigen PSI, Switzerland

[2]Lucerne University of Applied Sciences and Arts, School of Engineering and Architecture, Bioenergy Research, 6048 Horw, Switzerland

[3]Institute for Atmospheric and Climate Science, ETH, Zurich, Switzerland

[4]Aix Marseille Univ, CNRS, LCE, Marseille, France

Correspondence to: Josef Dommen (josef.dommen@psi.ch)

Abstract. Wood combustion emissions can induce oxidative stress in the human respiratory tract caused by reactive oxygen species (ROS), either directly or after oxidation in the atmosphere. To improve our understanding of the ROS generation potential of wood combustion emissions, a suite of smog chamber (SC) and potential aerosol mass (PAM) chamber experiments were conducted under well determined conditions for different combustion devices and technologies, different fuel types, operation methods, combustion regimes, combustion phases and aging conditions. The ROS content as well as the chemical properties of the aerosols were quantified by a novel ROS analyzer and a high resolution time of flight aerosol mass spectrometer (HR-ToF-AMS). For all eight tested combustion devices, primary ROS concentrations substantially increased upon aging. The level of primary and aged ROS emission factors (EF_{ROS}) were dominated by the combustion device (within different combustion technologies) and to a greater extent by the combustion regimes: the variability within one device was much higher than the variability of EF_{ROS} from different devices. Aged EF_{ROS} under bad combustion conditions were ~2-80 times higher than under optimum combustion conditions. EF_{ROS} from automatically operated combustion devices were on average one order of magnitude lower than those from manually operated appliances, which indicates that automatic combustion devices operated at optimum conditions to achieve near-complete combustion should be employed to minimize ROS emissions. The parameters controlling the ROS formation in secondary organic aerosol were investigated by employing a regression model, including the fractions of the mass spectrometric signatures *m/z* 44 and 43 in SOA ($f_{44\text{-}SOA}$ and $f_{43\text{-}SOA}$), the OH exposure, and the total organic aerosol mass. The regression model results of the SC and PAM chamber aging experiments indicate that the ROS content in SOA seems to increase with the SOA oxidation state, which initially increases with OH exposure and decreases with the additional partitioning of semi-volatile components with lower ROS content at higher OA concentrations, while further aging seems to

result in a decay of ROS. The results and the special data analysis methods deployed in this study could provide a role model for ROS analysis of further wood or any other combustion studies investigating different combustion conditions and aging methods.

1 Introduction

Numerous studies have shown a link between exposure to airborne particulate matter (PM) and worldwide morbidity and mortality (Beelen et al., 2013; Dockery et al., 1993; He et al., 2016), as well as a strong correlation of airborne PM with lung function (Lee et al., 2011; Pope et al., 2002; Adam et al., 2015; Hwang et al., 2015). The adverse health effects of PM are related to the aerosol chemical composition (Kelly and Fussell, 2012; Baltensperger et al., 2008). Residential wood combustion can contribute 5–44 % to the total ambient $PM_{2.5}$ (particulate matter with a diameter smaller than 2.5 μm), depending on the environment (Zhang et al., 2010; EPBE, 2005; USEPA, 2000; EEA, 2013a; Ciarelli et al., 2017). In addition to PM, wood combustion emits a wide range of gaseous pollutants, including volatile organic compounds, which upon oxidation can form secondary organic aerosol. Although wood is considered to be a climate neutral source of energy, epidemiological studies suggest that wood smoke may contribute significantly to premature mortality (Boman et al., 2003; Johnston et al., 2012), because of its association with respiratory disease, cerebrovascular diseases and impaired lung function (Liu et al., 2017; Yap, 2008; D. G. Fullerton, 2011). Liu et al. (2017) found a 7.2 % increase in the risk of respiratory hospital admissions during days with high wildfire-specific $PM_{2.5}$ compared to non-wildfire smoke event days. Exposure to wood combustion particles may cause moderate inflammatory activity, cell death and DNA damage, and adverse effects to airway epithelia (Krapf et al., 2017; Tapanainen et al., 2012; Muala et al., 2015; Marabini et al., 2017). These adverse effects may be related to oxidative stress caused by free radicals induced by inhaled PM, which overwhelms the antioxidants in the body (Lobo et al., 2010). In turn, free radical formation may be due to reactive oxygen species (ROS) present in atmospheric aerosol, transition metals undergoing Fenton reactions, or redox cycling organic compounds like quinones. The content of ROS in wood combustion emissions is largely unknown, with the contribution from secondary organic aerosol being particularly uncertain. This limits our understanding of the adverse health effects of wood smoke. Acellular assays enable the assessment of particulate ROS by methods that are easily applicable to field and laboratory studies. One such assay monitors the rapid decay of 2',7'-dichloorofluorescin (DCFH) to a fluorescent compound (DCF) in the presence of horseradish peroxidase (HRP) (King and Weber, 2013; Fuller et al., 2014b; Huang et al., 2016; Wang et al, 2011). The DCFH assay has been shown to be sensitive towards a broad range of ROS, and to have fast response rates and linear response to varying ROS concentrations, thus being suitable to evaluate the overall oxidative activity of PM (Zhou et al., 1997; Venkatachari and Hopke, 2008; King and Weber, 2013, Zhou et al., 2017).

Functionalized species formed from oxidation often have more deleterious effects on human health than parent analogues (Wang et al., 2007; Fu et al., 2012). Therefore, studies of both primary and aged wood combustion aerosols are needed to advance our understanding of their impact on human health. To investigate the aged aerosol products in a controlled and reproducible environment, atmospheric simulation systems such as smog chambers (SC) and potential aerosol mass (PAM) chambers are commonly used. In the present study, a suite of SC and PAM

experiments were conducted. As different types of wood, combustion appliances and combustion conditions result in varying levels of emissions (Johansson et al., 2004; Schmidl et al., 2011; Fitzpatrick et al., 2007; Heringa et al, 2011), eight wood combustion devices with variable combustion conditions were tested. Primary and aged biomass smoke generated under different combustion and aging conditions were characterized by an online ROS analyzer based on the 2',7'-dichlorofluorescin (DCFH) assay coupled with an aerosol collector. Observations from this study provide the more detailed evidence of the influence of combustion technology on the oxidative potential of the emitted PM compared to a previous similar study (Miljevic et al., 2010). We also show the variation of the ROS content from primary and aged aerosols under different operation conditions. Further, the contribution of reactive oxygen species to aged organic aerosol generated with different aging tools was investigated to clarify the ROS formation potential upon photo-oxidation. Results from these experiments may be directly compared with ambient measurements.

2 Experimental setup and methodology

We performed two sets of measurement campaigns, utilizing several wood combustion devices with different combustion conditions and two aging tools. First we present the different devices, then give a description of the PAM chamber and the Paul Scherrer Institute (PSI) mobile smog chamber (PSI-MSC, ~ 7 m^3) and the PSI stationary smog chamber (PSI-SSC, 27 m^3) (Platt et al., 2013, 2014; Paulsen et al., 2005), including the experimental procedures, and finally discuss the combustion conditions and measurement strategy. An experiment schematic is shown in Figure S1. The combustion devices, experiment aging tools, as well as the test aspects are listed in Table 1.

2.1 Combustion devices

Eight combustion devices with different technologies were tested, including a pellet boiler (PB, automatic), a moving grate boiler equipped with electrostatic precipitator (MGB, automatic), a updraft combustion pellet stove (PS, automatic), a two-stage combustion downdraft log wood boiler (LWB, manual), two advanced two-stage combustion log wood stoves (LWS1, manual, updraft; LWS2, manual, updraft combustion when cold and downdraft combustion when hot), and two conventional single-stage combustion log wood stoves (LWS3: manual, and LWS4: manual). In the following, we describe the different combustion devices.

PB. Automatically operated pellet boiler, with two-stage updraft combustion and a nominal heat output of 15 kW, using wood pellets (EN certified, moisture content 7 %) as the combustion fuel. Under optimum combustion conditions, the ideal air to fuel ratio (λ) is achieved leading to near-complete combustion and, consequently, the particle emissions are dominated by inorganic components which are contained in the pellets. The PB was also altered to enable the variation of the air to fuel ratio to investigate the influence of this parameter on the emissions. In this way, different combustion regimes could be achieved with this device, details are described in Sect. 2.2.

MGB. Automatically operated industrial moving grate boiler with nominal heat output of 150 kW, operated with wood chips (30 % moisture content). The grate has several zones where primary and secondary combustion air can be regulated.

Atmos. Chem. Phys. Discuss., https://doi.org/10.5194/acp-2017-1068
Manuscript under review for journal Atmos. Chem. Phys.
Discussion started: 21 November 2017

Atmospheric Chemistry and Physics Discussions

PS, LWB, LWS1, LWS2, LWS3 and LWS4. LWB, LWS1 and LWS2 are advanced stoves/boilers with two-stage combustion technology, while in LWS3 and LWS4 conventional single-stage updraft combustion is applied. PS is an automatically operated pellet stove with a nominal heat output of 6 kW under full load. It possesses a ventilator for the injection of the combustion air. However, due to a relatively simple air control, the PS is operated at high λ. We also investigated part load conditions at 3 kW. LWB, LWS1, LWS2, LWS3 and LWS4 are manually operated devices, with the norminal heat outputs of 30 kW, 8 kW, 4.6 kW, 8 kW and 4.5 kW, respectively. Further, the LWS1 is equipped with a storage container for logs, which slide on the grate due to gravity. For all four two-stage combustion devices (PS, LWB, LWS1, and LWS2) and one single-stage combustion device (LWS3), ROS emissions from starting, flaming and burn out phases were investigated (details of the combustion phases are described in Sect. 2.3). In the case of the LWS4, only the flue gas from the flaming phase was injected into the smog chamber, where the EF_{ROS} under different aging temperatures of -10 °C and 15 °C were tested. In three of the log wood operated devices (LWS1, LWS2 and LWS3) dry (13–16 % moisture content) and wet logs (24–42 % moisture content) were investigated. In the PS, wheat pellets (manufactured from milling residues, moisture content 9 %) were tested in addition to conventional wood pellets (EN certified, moisture content of 7 %). In the LWS4, beech wood logs with a moisture content of 18 ± 3 % were used.

Table 1. Overview of combustion devices and test aspects.

Aging conditions	Combustion devices	Test aspects
PAM chamber (T = ~38 °C, RH = 20 – 25 %)	Pellet boiler (PB)	EF_{ROS} of different burning regimes# (λ^{++}, λ^{-}, λ^{opt})
	Moving grate boiler (MGB)	EF_{ROS} of full/part load; With/without electrostatic precipitator (ESP)
	Pellet stove (PS)	EF_{ROS} of different burning phases**
	Log wood boiler (LWB)	EF_{ROS} of different burning phases**
	Log wood stove 1 (LWS1)	EF_{ROS} of different burning phases**
	Log wood stove 2 (LWS2)	EF_{ROS} of different burning phases**
	Log wood stove 3 (LWS3)	EF_{ROS} of different burning phases** Secondary ROS formation
PSI-MSC (~7 m^3) T = -10 or 15°C, RH = 50 %	Log wood stove 4 (LWS4)	Flaming phase, aging temperature; Secondary ROS formation
PSI-SSC (~ 27 m^3) Ambient T (22.5 °C), RH = 50 %	Log wood stove 4 (LWS4)	Flaming phase Secondary ROS formation

#,** The definitions of the burning regimes and burning phases are described in sect. 2.2.

2.2 Combustion conditions

Two parameters are used to describe the combustion conditions namely the combustion regimes and the combustion phases. Combustion regimes are defined by the air fuel equivalence ratio (λ) (Nussbaumer et al., 2000).

$$\lambda = \frac{O_{2,amb}[\%]}{O_{2,amb}[\%] - O_{2,flue\ gas}[\%]} \quad (1)$$

where $O_{2,amb}$ and $O_{2,flue\ gas}$ are the oxygen contents in ambient air ($O_{2,amb}$ = 21) and in the flue gas, respectively. Depending mainly on the level of excess air three combustion regimes are distinguished: lack of oxygen (λ^-), optimum combustion condition (λ^{opt}), and (high) excess of oxygen (λ^{++}). Each of these is characterized by a different type of combustion particles, i.e., comprising mostly soot, salts, and condensable organic compounds, respectively (Nussbaumer and Lauber, 2010). It should be noted that in wood combustion λ is always > 1. Consequently, λ^- and λ^{++} only describe λ-values which are clearly (for λ^{++} at least 1.5 fold or higher) below or above λ^{opt}.

The three combustion regimes were achieved by changing the air to fuel ratio in the pellet boiler (PB). Optimum combustion conditions (λ^{opt}) were easily achieved by operating the PB under the designed optimum operation mode. High excess of oxygen (λ^{++}) compared to λ^{opt} was obtained by additionally blowing air into the combustion chamber via the ignition tube. The lack of oxygen (λ^-) regime was obtained by manually closing the secondary combustion air inlet. It should be noted that in real life operation λ^{++} and λ^- conditions only occur with severe mal-operation. These conditions were investigated since they result in distinct emission characteristics (high NMVOC emissions during λ^{++} and high soot emissions during λ^- (Nussbaumer and Lauber, 2010).

In the MGB, part load (50 kW) and full load (150 kW) conditions were tested, as well as the influence of an electrostatic precipitator (ESP) installed downstream of the combustion unit. ESPs are widely used in both large and small scale wood combustion devices to reduce PM emissions (Bologa et al., 2011; Nussbaumer and Lauber, 2010).

Combustion phases in the log wood stoves, log wood boiler and pellet stove were classified using the modified combustion efficiency (MCE), defined as the molar ratio of the emitted CO_2 divided by CO plus CO_2 ($CO_2/(CO+CO_2)$), in the flue gas after wood combustion (Ward and Radke, 1993). Each full combustion cycle includes three combustion phases: start phase (beginning of the burning cycle before MCE reaches 0.974), flaming phase (between start and burnout phase, with MCE > 0.974) and burnout phase (after flaming phase, with MCE < 0.974). As mentioned in Sect. 2.1, all three phases were obtained in the PS, LWB, LWS1, LWS2 and LWS3. In the PS, LWB and LWS1, experiments started with a cold start, followed by a flaming phase and burn out. In the LWS2 and LWS3, after the first complete combustion cycle starting with a cold start, several full combustion cycles followed by adding new logs into the combustion chamber after the burn out was finished (warm start). In devices where the combustion phases were rapidly changing the ROS analyzer was not able to separate these combustion phases due to a slow response time (~ 8 min). Consequently, the single combustion phases, including the start, flaming and burn out, as well as the combined combustion phases start + flaming or flaming + burn out were used for the ROS analysis. In the LWS4, with which the experiments were conducted in the PSI-MSC (at temperatures of 263 K and 288 K), and the PSI-SSC (at a temperature of 288 K), only emissions from the flaming phase were sampled.

2.3 Experimental procedures and aging tools

2.3.1 PAM chamber

Seven combustion devices (except LWS 4) were tested using the PAM chamber as an aging tool. The emissions were sampled through a heated line (473 K), diluted by a factor of ~100-150 using two ejector diluters in series (VKL 10, Palas GmbH), and then injected into the PAM chamber (see Figure S1 in the Supporting Information). The original concept of the PAM chamber is described by (Kang et al., 2007). Briefly, the PAM chamber is a single, 0.015 m^3 cylindrical glass chamber, flanked by two UV lamps. Prior to entering the PAM chamber, pure air (1.6 L min^{-1}, humidified with a Nafion membrane, Perma Pure LLC) used as an OH precursor and a stream of diluted d9-butanol (98%, Cambridge Isotope Laboratories) were merged with the incoming reactant flow. The OH exposure during aging was defined as the integral of the OH concentration over the reaction time, and was calculated from the decay of the d9-butanol, measured by a proton transfer reaction–mass spectrometer (PTR-MS 8000, Ionicon Analytik GmbH) (Barmet et al., 2012). The total flow rate in the PAM chamber was maintained at ~ 7 L min^{-1}, which was the sum of the flow rates of the instruments and a supplementary flow, resulting in a residence time of approximately 2 minutes. The OH exposure was controlled by adjusting the UV light intensity to obtain different OH concentrations. An outer ring flow (~0.7 L min^{-1}), which was discarded, was used to minimize wall losses and the instrument sampled only from the inner flow of the PAM chamber (~6.3 L min^{-1}). The temperature in the PAM chamber was around 38 ^{o}C due to the lamps. Primary wood combustion emissions were characterized either before or after the PAM chamber when the lights were switched off. Aged emissions were characterized after the PAM chamber with lights on. All the experiments were conducted under OH exposures of (1.1-2.0)×10^8 molec cm^{-3} h which corresponds to ~ 4.5-8 days of aging in ambient by assuming a mean daily OH concentration of 1×10^6 molec cm^{-3}. The applicability of the PAM chamber to measure wood combustion emissions has been shown in a previous study (Bruns et al., 2015).

2.3.2 Smog chamber aging

The second set of experiments was conducted in the PSI mobile smog chamber (PSI-MSC, ~ 7 m^3) at temperatures of 263 K and 288 K, and the PSI stationary smog chamber (PSI-SSC, 27 m^3) at 295.5 K. An overview of the experimental setup is also shown in Figure S1. Generally, 3 pieces of dry beech logs, 4 pieces of kindling and 3 fire starters and 9 pieces dry beech logs, 8 pieces kindling and 4 fire starters were combusted in LWS4 for average (2.9 ± 0.3 kg) and high (5.1 kg) load experiments, respectively (details in Sect. 2.1). The wood moisture content was 19 ± 2 %. Only emissions during the flaming phase with a modified combustion efficiency (MCEs) in the range from 0.974 to 0.978 were sampled. Emissions were sampled for 11-21 min and injected into the PSI-MSC using an ejection diluter, yielding a total dilution factor of 100 to 200. Hydroxyl radical (OH) concentrations in the chamber are controlled by continuous injection of nitrous acid into the smog chamber (after the characterization of the primary emissions as described below in Sect. 3.1), which produces OH upon irradiation by UV lights (Platt et al., 2013). The OH exposure was estimated by monitoring the decay of d9-butanol (butanol-D9, 98%, Cambridge Isotope Laboratories) following a single injection before the UV lights were turned on. In all five experiments conducted in the PSI-MSC, the aging time lasted 4.5-6 h. The OH exposure was 2.6-4.8×10^7 molec cm^{-3} h which corresponds to ~1-2 days of aging in ambient by assuming a mean daily OH concentration of 1 × 10^6 molec cm^{-3}. More details about some of the PSI-MSC experiments of this campaign can also be found in Bruns et al. (2016, 2017). One

Atmos. Chem. Phys. Discuss., https://doi.org/10.5194/acp-2017-1068
Manuscript under review for journal Atmos. Chem. Phys.
Discussion started: 21 November 2017

additional experiment was conducted in the PSI-SSC, with an OH exposure up to 4.0× 10^8 molec cm^{-3} h, equivalent to ~17 days of aging assuming a mean daily OH concentration of 1 × 10^6 molec cm^{-3}, extending the aging range beyond the range achieved by the PAM chamber (~1-8.5 days).

2.4 Particle phase characterization

The non-refractory particle chemical composition was measured using a high resolution time-of-flight aerosol mass spectrometer (HR-ToF-AMS, flow rate: 0.1 L min^{-1}, Aerodyne Research Inc.) (DeCarlo et al., 2006). The HR-ToF-AMS measured the total organic aerosol (OA), SO_4^{2-}, NO_3^-, NH_4^+, Cl^-, as well as the two most dominant oxygen-containing ions in the OA spectra, Org44 (mostly CO_2^+) and Org43 (mainly $C_2H_3O^+$ for the oxygenated OA and $C_3H_7^+$ for the hydrocarbon-like OA) (Ng et al., 2011). Equivalent black carbon (eBC) was determined using an Aethalometer (AE33, Magee Scientific; flow rate: 2 L min^{-1}, Drinovec et al., 2015).

The oxidative potential of the aerosol particles was characterized by an on-line ROS analyzer (flow rate: 1.7 L min^{-1}) (Zhou et al., 2017). The aerosols particles were collected in a mist chamber type aerosol collector, dissolved into water and mixed with a 2',7'-dichlorofluorescin (DCFH)/horseradish peroxidase solution. The ROS converts DCFH to DCF, which is detected by fluorescence and quantified as nM-H_2O_2 equivalents. The time resolution of the on-line ROS analyzer was ~ 8 minutes, preventing resolving brief discrete combustion phases. Therefore, different methods were used to calculate the average ROS emissions under different conditions:

1) average (Figure S2a): utilized when the combustion conditions were relatively stable and sufficiently long to yield a stable ROS signal;

2) integrated average (Figure S2b): in cases of variable combustion conditions, the ROS signal was integrated over the measurement period which could include one or several phases from the same burn;

3) extrapolation + integrated average (Figure S2: panels 2c_1 and c_2): when the combustion conditions were variable and the background could not be measured between two combustion conditions due to the time resolution of the ROS instrument. We extrapolate each measurement to the background value and then make the integrated average calculation as described above.

The various definitions for ROS and related aerosol characteristics are presented below:

ROS emission factors *(EF_{ROS}).* ROS emission factors (EF_{ROS}) were calculated as the amount of ROS in nmol-H_2O_2 equivalents per kilogram wood burnt, using Eq. (2):

$$EF_{ROS} = \frac{n_{ROS}}{M_c} C_{wood} \cong \frac{[n_{ROS}]}{\sum([\rho C_{CO_2}]+[\rho C_{CO}]+[\rho C_{CH_4}]+[\rho C_{VOC}]+[\rho C_{eBC}]+[\rho C_{OC}])} C_{wood} \quad (2)$$

where $[n_{ROS}]$ is the background-corrected concentration of ROS (nmol m^{-3}) in the emitted particles either before (primary ROS) or after aging (aged ROS), $[\rho C_x]$ are the carbon mass concentrations calculated from the background-corrected, carbon-containing species where x includes CO_2, CO, CH_4, volatile organic compounds (VOC), eBC, and particulate organic carbon (OC). M_C is the carbon mass burnt and C_{wood} represents the average

carbon fraction of the wood fuel, ~ 0.46, measured in this study using an elemental analyzer. OC data were obtained from AMS measurements. Similarly, the organic aerosol (OA) emission factors (EF_{OA}) were calculated by replacing the ROS concentration by OA.

ROS fraction. In order to study the ROS formation during aging, the secondary ROS fraction ($f_{ROS\text{-}SOA}$) is introduced. It expresses the amount of secondary ROS (ROS_S = aged ROS –primary ROS) per amount of secondary organic aerosol (SOA) formed during aging and as calculated from Eq. (3)

$$f_{ROS-SOA} = \frac{ROS_S}{SOA} \quad (3)$$

Secondary organic aerosol (SOA) and secondary ROS (ROSs) were calculated by subtracting primary organic aerosol (POA) and primary ROS (ROSp) from the total OA and aged ROS, respectively, assuming ROSp and POA to be only lost to the chamber wall at the same rate as eBC but otherwise to remain constant during aging. Although both quantities may not be conserved, a decrease of both does partially compensate in the ROS fraction. In the SC experiments, POA is defined as the OA mass before lights on, while SOA is estimated as the difference between total OA and the time dependant POA mass accounting for particle wall loss. Wall loss rates for POA and SOA were assumed to be the same as that of the measured eBC. In PAM aging experiments, each experiment had a certain POA (measurements before PAM or after PAM with lights of) and SOA (measurements after PAM with lights on).

$f_{44\text{-}SOA}$ and $f_{43\text{-}SOA}$. To express the degree of oxygenation of SOA, the fraction of secondary Org44 and Org43 in SOA (represented as $f_{44\text{-}SOA}$ and $f_{43\text{-}SOA}$) is introduced, which is calculated from Eq. (4)

$$f_{44-SOA} = \frac{Org_{44-SOA}}{SOA};\ f_{43-SOA} = \frac{Org_{43-SOA}}{SOA} \quad (4)$$

where $Org_{44\text{-}SOA}$ is the difference of total Org44 and primary Org44, $Org_{43\text{-}SOA}$ is the difference of total Org43 and primary Org43 and using the same procedure as for the SOA calculation mentioned above.

Wall loss correction. The wall loss correction in the SC was done by assuming the same losses for all particle components as for the inert tracer eBC. The wall loss corrected concentration of OA or ROS (X) can be derived using the equation Eq. (5):

$$X_{WLC}(t) = X_{meas}(t) \times \frac{BC(t0)}{BC(t)} \quad (5)$$

where $X_{meas}(t)$ refers to the concentration of X measured at time t. BC (t_0) and BC (t) are the concentrations of BC when lights were switched on and at time t, respectively.

2.5 Gas phase characterization

During the PAM chamber experiments, total volatile organic compounds (VOC) and CH_4 (using a flame ionization detector (FID) with a non-methane cutter, model 109A, J.U.M Engineering), CO and NO (with a non-dispersive infrared analyzer, Ultramat 23 Siemens) as well as O_2 (using a paramagnetic oxygen analyzer, Ultramat 23 Siemens)

were determined in the hot undiluted flue gas. In SC aging experiments CO was measured with a cavity ring-down spectrometer (G2401, Picarro, Inc.). In all experiments, the composition of VOCs was determined by a proton transfer reaction–mass spectrometry (PTR-MS 8000, Ionicon Analytik GmbH). For CO_2 a cavity ring-down spectrometer (G2401, Picarro, Inc.) was used in the SC aging experiments and a non-dispersive infrared (NDIR) analyzer (model LI-820, LI-COR®) in the PAM chamber aging experiments.

3 Results and discussion

3.1 Primary and aged ROS emission factors (EF_{ROS})

The ROS and OA emission factors are presented in Table 2 for all combustion condition, together with the number of tests, the combustion efficiency (MCE), the air to fuel ratio (λ), and the aerosol bulk properties determined with the AMS (OM:OC, O:C and H:C ratios). The given values are the 25 percentile and 75 percentile of averages from several experiments and the data points considered for the calculations were restricted to the time period of the ROS measurements. As shown in Fig. 1, ROS emission factors (EF_{ROS}) for primary and aged OA were highly variable depending on the combustion conditions and devices. For all devices and combustion conditions, a substantial enhancement in the EF_{ROS} is observed with aging, indicating the importance of secondary ROS production. The ROS enhancement factor, defined as the ratio between aged and primary EF_{ROS}, range between 4 and 20, with lower values for MGB (~ 4) and PB under λ^{opt} combustion condition (~ 6), and higher values for PB under λ^{-} and λ^{++} combustion conditions (> 10). The ROS enhancement factors for all log wood stoves as well as LWB are comparable, with an average value around 10.

The variability in the EF_{ROS} in primary and aged OA for one device is much higher than the variability between average emission factors for different devices, spanning almost two orders of magnitudes. Despite this, EF_{ROS} from PB and MGB (80-8 890 nmol kg^{-1} wood and 2 440-1.83×10^5 nmol kg^{-1} wood for primary and aged emissions, respectively) are on average one order of magnitude lower than those from PS, LWB and LWS1-4 (220-1.89×10^6 nmol kg^{-1} wood and 3 570-1.1×10^6 nmol kg^{-1} wood for primary and aged emissions, respectively). These results clearly indicate differences due to the combustion technology, as a general rule, EF_{ROS} were lowest for automatically operated devices and higher for manually operated devices: PB and MGB are automatically operated and the primary and secondary air supply as well as the fuel feeding is controlled permanently, while LWB and LWS1-4 are manually operated. The PS is automatically operated but is operated at high λ and exhibits similar EF_{ROS} to the manual devices. Part of the EF_{ROS} variability within each device can be ascribed to the combustion phase, with higher emission factors for the starting and burn out phases compared to the flaming/stable phase. This is especially true for the aged emissions from the PS (EF_{ROS} of the start phases was on average 13 times higher than the flaming phase; Mann-Whitney *p*-value = 0.06), the LWS2 (EF_{ROS} of the start phases was on average 1.7 times higher than the flaming phase, Mann-Whitney *p*-value = 0.24, not significant) and the LWS3 (EF_{ROS} of the start and burn out phases were on average 1.5 times higher than the flaming and flaming + burn out phase, Mann-Whitney *p*-value = 0.07).

For the automatically operated MGB, the primary EF_{ROS} did not statistically differ between part and full load operation (Mann-Whitney *p*-value = 0.95). However, the aged EF_{ROS} was a factor of ~3 higher for part load than for full load (Mann-Whitney, p-value = 0.23). The use of the electrostatic precipitator had little effect on the primary and aged ROS emissions, with the differences being within burn-to-burn variability.

For PB, the combustion operation could be systematically varied to investigate the influence of air to fuel ratio on ROS and OA emission factors before and after aging. The EF_{ROS} were highest under λ^{++} condition for both primary and aged emissions, with average values of 4 100 and 5.8×10^4 nmol kg^{-1} wood burnt, respectively (Fig. 1 and Table 2). Primary ROS emissions under λ^{opt} conditions did not statistically differ from λ^{-} conditions (Mann-Whitney, *p*-value = 0.43), but on average 7 and 3 times lower than that obtained under λ^{++} condition, respectively (Mann-Whitney, *p*-value < 0.005 for both cases). The aged EF_{ROS} under λ^{opt} and λ^{-} were also quite similar (Mann-Whitney, *p*-value = 0.20), but with average values 8 and 5.5 times lower than obtained under λ^{++} conditions, respectively (Mann-Whitney, *p*-value = 0.02 for both cases). This shows that the air to fuel ratio has a significant effect on the ROS emissions, which will be investigated for all devices hereafter.

Atmos. Chem. Phys. Discuss., https://doi.org/10.5194/acp-2017-1068
Manuscript under review for journal Atmos. Chem. Phys.
Discussion started: 21 November 2017

Atmospheric Chemistry and Physics Discussions

325 **Table 2.** Characterization of primary emissions from PAM chamber and SC aging experiments*

Devices	Test aspects		Number of tests	MCE	λ	ROS nmol kg^{-1}	Total PM mg kg^{-1}	Org mg kg^{-1}	OM:OC	O:C	H:C
PB	λ^{-}		3	[0.991, 0.992]	[1.29, 1.30]	[345, 882]	[246, 301]	[56, 62]	[2.1, 2.4]	[0.7, 0.9]	[1.3, 1.4]
	λ^{opt}		7	[0.999, 0.999]	[1.59, 1.64]	[288, 2325]	[50, 69]	[22, 29]	[2.7, 2.8]	[1.1, 1.2]	[1.3, 1.4]
	λ^{++}		15	[0.963, 0.983]	[3.02, 3.11]	[1940, 5944]	[33, 61]	[15, 26]	[2.5, 2.6]	[0.9, 1.0]	[0.9, 1.0]
MGB	Full load	Before ESP	5	[0.999, 0.999]	[1.99, 2.04]	[1758, 2034]	[65, 100]	[27, 48]	[3.1, 3.1]	[1.4, 1.4]	[1.1, 1.3]
		After ESP	3	[0.999, 0.999]	[3.91, 3.99]	[775, 1098]	[3, 4]	[1, 2]	[2.3, 2.7]	[0.7, 1.0]	[1.2, 1.4]
	Part load	Before ESP	6	[0.999, 0.999]	[2.12, 2.30]	[780, 4083]	[19, 25]	[8, 9]	[2.1, 2.3]	[0.6, 0.8]	[1.1, 1.3]
PS	All burning phases		5	[0.989, 0.995]	[4.97, 7.59]	[5376, 36415]	[204, 625]	[60, 427]	[2.2, 2.5]	[0.8, 1.0]	[1.1, 1.3]
LWB			20	[0.904, 0.999]	[1.47, 2.49]	[4307, 27590]	[262, 741]	[111, 277]	[2.5, 2.9]	[1.0, 1.4]	[1.1, 1.2]
LWS1			6	[0.850, 0.933]	[3.57, 7.05]	[5915, 52528]	[381, 572]	[142, 379]	[2.3, 2.4]	[0.9, 1.0]	[1.2, 1.2]
LWS2			6	[0.948, 0.976]	[3.51, 4.31]	[141457, 249755]	[49, 98]	[49, 98]	[2.3, 2.4]	[0.9, 1.0]	[1.2, 1.3]
LWS3			19	[0.930, 0.968]	[4.61, 9.57]	[12160, 61258]	[151, 356]	[14, 55]	[1.9, 2.1]	[0.5, 0.6]	[1.4, 1.6]
LWS4	Flaming		5	[0.972, 0.975]	[3.0, 3.6]	[37766, 57403]	[171, 440]	[83, 162]	[1.6, 1.7]	[0.30, 0.45]	[1.3, 1.5]

* Values of each parameter are described as [a, b], where a and b represent the 25th and 75th percentile of the averages from several experiments and the data points considered for the calculations were restricted to the time period of the ROS measurements

Atmos. Chem. Phys. Discuss., https://doi.org/10.5194/acp-2017-1068
Manuscript under review for journal Atmos. Chem. Phys.
Discussion started: 21 November 2017

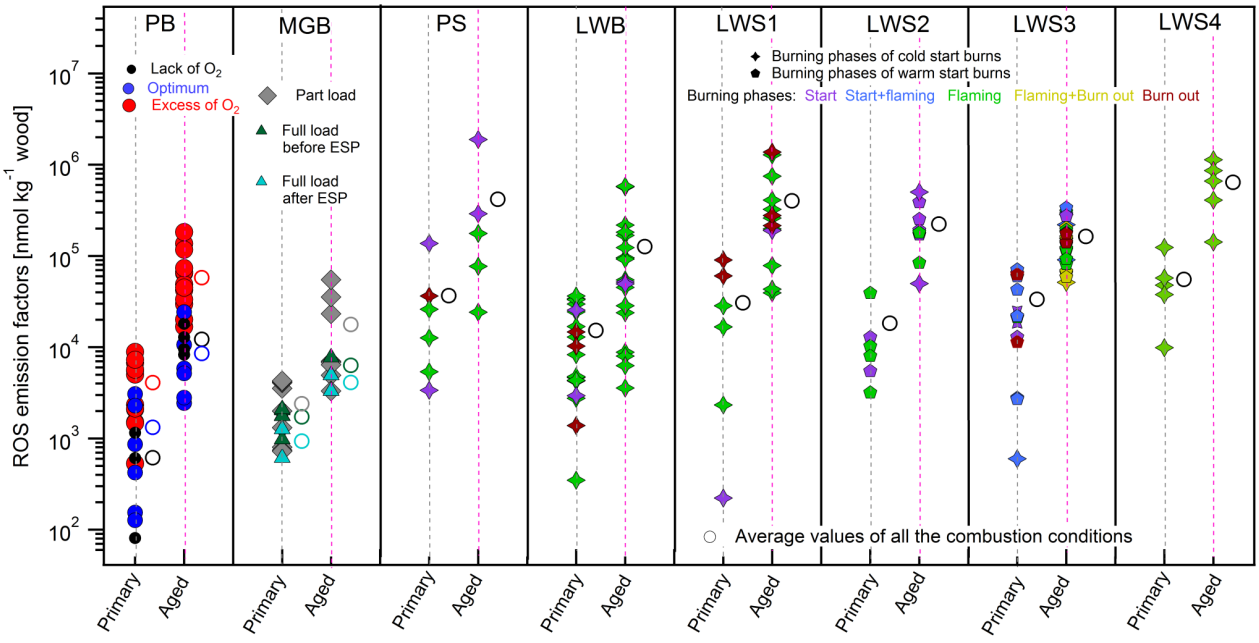

330 **Figure 1.** ROS emission factors (EF_{ROS}) for all tested combustion devices under different operating and aging conditions. Open circles symbols represent the average values of all the experimental data points for each condition. PB denotes Pellet boiler; MGB Moving grate boiler; PS Pellet stove; LWB Log wood boiler; LWS*n* Log wood stove n (*n* = 1, 2, 3, 4). Each data point represents one experiment. For each device, primary EF_{ROS} appear on the left side (gray dashed line) and aged EF_{ROS} on the right side (pink dashed line)

Atmos. Chem. Phys. Discuss., https://doi.org/10.5194/acp-2017-1068
Manuscript under review for journal Atmos. Chem. Phys.
Discussion started: 21 November 2017

Atmospheric Chemistry and Physics Discussions

3.2 EF_{ROS} under different combustion regimes

Fig. 2 shows the aged EF_{ROS} of the eight devices as a function of λ. Similar to PB, as already described above, a clear increase of EF_{ROS} in the aged aerosol can be observed with increasing λ values, with ~2-80 times higher aged EF_{ROS} values under bad combustion conditions than under optimum combustion conditions, although the extend of the increase and the overall trend were not the same for all individual devices. In the MGB all the burns occurred at $2.0 < \lambda < 2.2$, leading to aged EF_{ROS} in line with those from the PB between λ^{opt} (λ = 1.6) and λ^{++} (λ ranged from 2.7-3.4). The combustion in all stoves (PS, LWS1-4) exhibited higher λ ($\lambda > 2.2$) due to a less controlled air supply leading to less efficient combustion. In this excess of oxygen range, aged EF_{ROS} ranged between 1.68×10^4 nmol kg^{-1} wood and 1.38×10^6 nmol kg^{-1} for λ values between 2.2-17.6, where all aged EF_{ROS} were high but without any systematic trend with λ, suggesting that other parameters may influence ROS emissions as well. The LWB follows a different trend, where the aged EF_{ROS} increase sharply with λ, starting at lower λ values than the other manually operated devices. Aged EF_{ROS} for LWB ranged from 3530 to 5.79×10^5 nmol kg^{-1} wood within the λ-range of 1.5-2.6. Although trends in Fig. 2 show differences between devices, they highlight quite readily the important influence of the combustion conditions on aged EF_{ROS}.

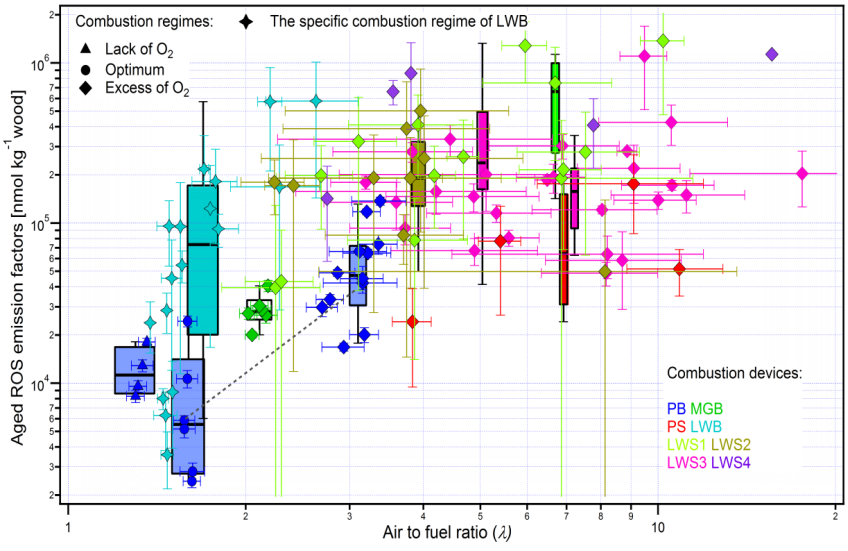

Figure 2. Aged ROS emission factors (EF_{ROS}) from different combustion regimes and combustion devices. The grey dashed line represents the EF_{ROS} increase with λ for the PB. The error bars of the y-axis of the data points denote the propagation of the uncertainty ($\delta = \sqrt{{\delta_1}^2 + {\delta_2}^2}$, with δ_1 and δ_2 representing the standard deviation of the averaged aged ROS and aged OA of the measurement time periods, respectively.); the error bars of the x-axis of the data points denote the standard deviation of the averaged aged λ of the measurement time periods.

While the combustion efficiency was found to have a strong influence on aged EF_{ROS}, the latter varies considerably, by a factor of 3-50, within the same combustion regime but for different combustion devices. In Fig. 3, we investigate to which extent this variability in aged EF_{ROS} is related to the variability in the bulk OA emissions. The high correlation (Pearson's R = 0.92) observed in Fig. 3 suggests that changes in aged EF_{OA} explain a great fraction of the variability in aged EF_{ROS}, implying that this variation is inherent to wood

Atmos. Chem. Phys. Discuss., https://doi.org/10.5194/acp-2017-1068
Manuscript under review for journal Atmos. Chem. Phys.
Discussion started: 21 November 2017

Atmospheric Chemistry and Physics Discussions

combustion conditions. Nonetheless, additional unexplained variation was observed between the two variables in Fig. 3, with the aged ROS emission factors varying by a factor of 2.6 on average for the same aged EF_{OA}. To elucidate the reasons behind this variability, we investigate in the following the parameters controlling the secondary ROS formation and its content in OA upon aging.

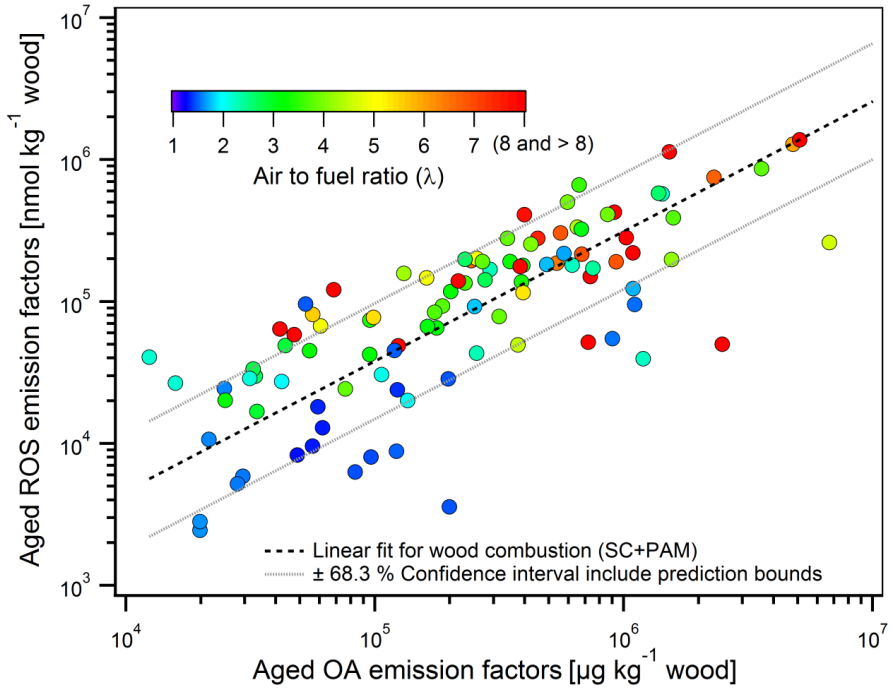

Figure 3. Aged ROS emission factors vs. aged OA emission factors. Marker color correspond to the air to fuel ratio (λ). Fitting equation: $\log_{10}(EF_{ROS}) = 0.92\log_{10}(EF_{OA})$ indicating that the relationship between aged ROS and aged OA is almost linear. The geometric standard deviation obtained from the fit is 2.6, suggesting that the aged ROS content of aged OA may vary significantly depending on the combustion and atmospheric aging conditions.

3.3 Influence of aging conditions on ROS formation

Atmos. Chem. Phys. Discuss., https://doi.org/10.5194/acp-2017-1068
Manuscript under review for journal Atmos. Chem. Phys.
Discussion started: 21 November 2017

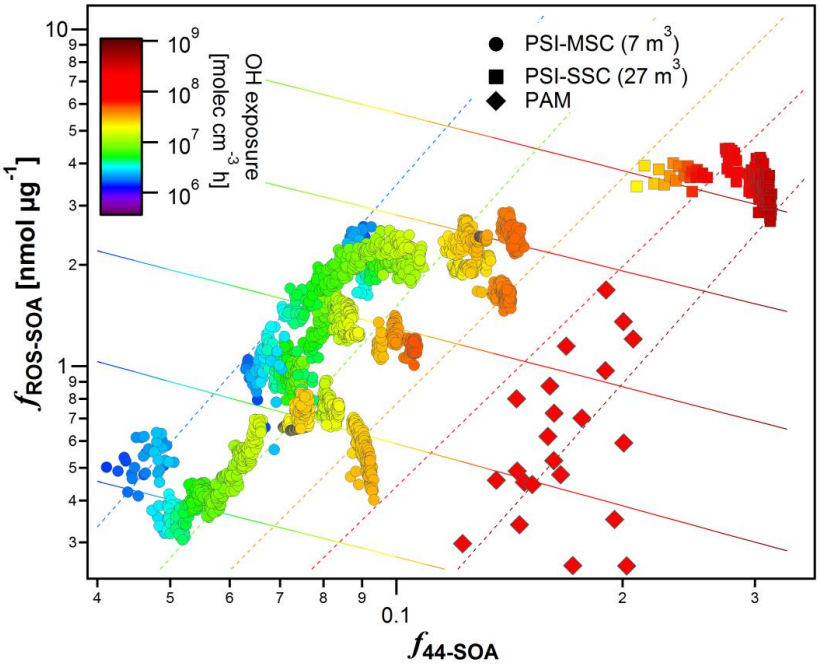

Figure 4: Variation of the fraction of ROS in SOA, $f_{ROS\text{-}SOA}$, with the fraction of *m/z* 44 in the total signal SOA as measured by the AMS ($f_{44\text{-}SOA}$) color coded with the OH exposure estimated from the decay of d9-butanol measured by the PTR-ToF-MS. Data are collected from two different smog chambers (SC) and from the PAM chamber. Dashed lines are isopleths of constant OH exposures, while solid lines are obtained by isolating the effect of OH exposure from other variables. To help discerning different experiments performed in SC, the same content in this figure is plotted again in Fig. S3, where those SC experiments are labeled by different numbers.

Regression model setup and performance. In this section, we seek to evaluate the relationship between the fraction of ROS in SOA, $f_{ROS\text{-}SOA}$, and parameters controlling its formation. To exclude the influence of the combustion devices, the data obtained using the LWS4 in the SC experiments and using the LWS3 in the PAM chamber experiments was chosen for the analysis, as the LWS3 and LWS4 are both conventional single-stage combustion devices. Four different parameters were investigated, including $f_{43\text{-}SOA}$ and $f_{44\text{-}SOA}$, the OH exposure, and the organic aerosol mass, by running the regression model as follows:

$$f_{ROS-SOA} = a \times SOA + b \times f_{44-SOA} + c \times f_{43-SOA} + d \times (OH\ exposure) + intercept \quad (6)$$

$f_{43\text{-}SOA}$ and $f_{44\text{-}SOA}$ are believed to represent the contributions of moderately oxygenated components (e.g. alcohols and carbonyls) and highly oxygenated components (e.g. carboxylic acids and peroxides), respectively. The organic aerosol mass may influence the fraction of ROS in SOA, by affecting the amount of condensing semi-volatile species, which might be characterized by different $f_{ROS\text{-}SOA}$ compared to low-volatility species dominating at low organic aerosol mass. The aim of the multiple regression analysis used here is to extract the influence of different aging factors on the observed variance in $f_{ROS\text{-}SOA}$ (the 2.6 factor variance described in Fig. 3), and to assess the magnitude of their influence. We do, however, not seek to propose using the model and the model coefficients for a deterministic explanation of ROS formation.

Since the dependent variable, $f_{ROS\text{-}SOA}$, and the predictors considered are lognormally distributed – typical of concentrations and contributions –, we have log-transformed the data before the multiple regression analysis. We note though that this step did not influence the conclusions of the analysis, as a multi-linear model applied to the raw data without a prior log-transformation suggests a similar relationship between $f_{ROS\text{-}SOA}$ and the predictors. Both models reasonably represented the measurements (~ 20 % error, Fig. S4), but log-transforming the data allowed for a better capturing of lower $f_{ROS\text{-}SOA}$ and a less skewed distribution of the model residuals (Fig. S4). We did not consider any interactions between the different regressors, as this is taken into account through the prior log-transformation of the data. For the parameterization, we only considered the SC data and will discuss whether the PAM chamber data could be satisfactorily explained by the same parameterization or whether the amount of ROS formed under different conditions, with high OH concentrations in the PAM chamber, is different.

We note that the different predictors exhibit some degree of collinearity. For example, not unexpectedly, $f_{44\text{-}SOA}$ significantly increases with aging (R^2 between $f_{44\text{-}SOA}$ and OH exposure = 0.68), while $f_{43\text{-}SOA}$ increases with the amount of organic aerosol in the smog chamber (R^2 = 0.56), possibly due to the enhanced partitioning of the moderately oxidized organic species at higher absorptive mass (Pfaffenberger et al., 2013). Both variables, $f_{44\text{-}SOA}$ and $f_{43\text{-}SOA}$, are slightly inversely correlated (R^2 = 0.26). Therefore, prior to the regression analysis we inspected the severity of multicollinearity by computing the variance inflation factors (VIF) for all four predictors. All VIF values were between 2.5 and 6 (highest for f_{44}-SOA and for OH exposure), indicating a moderate degree of multicollinearity (VIF values above 10 would be related to excessive multicollinearity). While a direct consequence of multicollinearity is an increased probability of erroneously rejecting the dependence of $f_{ROS\text{-}SOA}$ on one of the factors, a type two error, the regression analysis suggests that the dependence of $f_{ROS\text{-}SOA}$ on all parameters is significant ($p < 10^{-6}$).

Model results for SC data. The correlation between $f_{ROS\text{-}SOA}$ and the most important regressors is shown in Fig. 4. The analysis suggests that the greatest share of explained variability in $f_{ROS\text{-}SOA}$ could be attributed to $f_{44\text{-}SOA}$. An increase in $f_{44\text{-}SOA}$ by one geometric standard deviation (a factor of 1.45) resulted in our case in a doubling of the secondary ROS fraction ($f_{ROS\text{-}SOA}$). This indicates that more oxygenated compounds are preferentially ROS active compared to others.

The second most important parameter controlling the secondary aerosol ROS content under our conditions is found to be the OH exposure. An increase in OH exposure by one geometric standard deviation (a factor of 2.7) resulted in our case in a 60 % decrease of the ROS fraction in SOA ($f_{ROS\text{-}SOA}$). We note that the considerable effect size of this variable stems from its large variability, spanning a dynamic range of 2.5 orders of magnitudes (e.g. ~ 4 times more variation in OH exposure compared to $f_{44\text{-}SOA}$ would be required to achieve the same effect on $f_{ROS\text{-}SOA}$). The anti-correlation between OH exposure and $f_{ROS\text{-}SOA}$ indicates that the initially formed ROS are prone to further reactions, consistent with previous observations of rapid peroxide (Krapf et al., 2016) and ROS (Zhou et al., 2017) decay. The mechanism by which ROS evolves remains uncertain, but may involve the oxidation of ROS related molecules by OH as well as their photolysis and unimolecular decay reaction. We note that the OH exposure increases the oxidation state of the aerosol, here represented by $f_{44\text{-}SOA}$, thereby indirectly

increasing the ROS content, especially in the beginning of the experiment. Therefore, the actual effect of OH exposure on $f_{ROS\text{-}SOA}$ could only be revealed when it was isolated from the $f_{44\text{-}SOA}$ effect (see Fig. 4).

The analysis suggests that $f_{43\text{-}SOA}$ and the organic mass concentrations exhibit a low, but statistically significant, effect on $f_{ROS\text{-}SOA}$ (Fig. S5). Their increase results in a decrease in the secondary ROS content, consistent with the increased partitioning of moderately oxygenated components, which seem to contain less ROS.

Comparison between SC and PAM chamber data. The conditions in the PAM chamber are different from those in the SC. PAM chamber experiments were conducted at high OH exposures of ~10^8 molecules cm^{-3} h, where the resulting aerosol was highly oxygenated. However, the secondary ROS content of the aerosol in the PAM chamber was largely within the expected range, following consistent trends with high OH exposures and high $f_{44\text{-}SOA}$ as in the SC (Fig. 4). We examined in more detail whether the regression model parameters obtained from the SC could faithfully represent the $f_{ROS\text{-}SOA}$ measured in the PAM chamber. Indeed, the model was capable to predict, within uncertainties (2σ), the $f_{ROS\text{-}SOA}$ measured in the PAM chamber for low organic aerosol concentrations (average 21 µg m^{-3}), but considerably (factor of three on average) overestimated $f_{ROS\text{-}SOA}$ at higher concentrations (average 68 µg m^{-3}). This is because such a range of concentrations at high OH exposures and high $f_{44\text{-}SOA}$ was not included in the training dataset, and as a result the model slightly underestimated the effect of OA concentration on $f_{ROS\text{-}SOA}$ (e.g., a three-fold increase in OA concentration in the PAM chamber results in a decrease of $f_{ROS\text{-}SOA}$ by 45 %, while the model suggests that the same increase would only result in a 10 % decrease). Despite this, for similar conditions $f_{ROS\text{-}SOA}$ measured in the PAM chamber and the SC were similar within our uncertainties. We also note that this slight bias does not affect the main conclusions of the analysis: the secondary ROS content seems to initially increase with the SOA oxidation state, which increases with OH exposure and decreases with the additional partitioning of semi-volatile components with lower secondary ROS content at higher SOA concentrations, while further aging seems to result in a decay of ROS.

4 Summary and Conclusions

In this study, eight wood combustion devices for log wood, pellets and wood chips, denoted as log wood boiler (LWB), log wood stove 1 (LWS1), log wood stove 2 (LWS2), log wood stove 3 (LWS3) and log wood stove 4 (LWS4), pellet boiler (PB), pellet stove (PS) and moving grate boiler (MGB), were tested. Experiments were conducted in a suite of aging tools, including the Paul Scherrer Institut mobile smog chamber (PSI-MSC, ~ 7 m^3, OH exposure: (2.6-4.8)×10^7 molec cm^{-3} h), the Paul Scherrer Institut stationary smog chamber (PSI-SSC, 27 m^3, OH exposure: (0.13-40)×10^7 molec cm^{-3} h), and the potential aerosol mass chamber (PAM chamber, OH exposure: (11-20)×10^7 molec cm^{-3} h) to investigate the ROS formation potential of primary and aged wood combustion emissions from different combustion devices and conditions. The influence of combustion technologies, wood types (wood logs, wood pellets and wood chips), operation type (e.g. with/without ESP, automatic vs. manual operation), combustion regime (different air to fuel ratio (λ) ranging from low (λ^-), to optimum (λ^{opt}) and high values (λ^{++})), combustion phases (start, flaming, burn out) and aging conditions (SC aging/PAM chamber aging) to ROS emission factors (EF_{ROS}) were investigated. Results show that EF_{ROS} for primary and aged OA were highly variable depending on the combustion conditions and devices. For all devices and combustion conditions, EF_{ROS} substantially increased upon aging, indicating the secondary production of

ROS. The ROS enhancement factors ranged between 4 and 20, with lower values for the MGB (~ 4) and PB under λ^{opt} combustion condition (~ 6), and higher values for the PB under λ^{-} and λ^{++} combustion conditions (> 10). The ROS enhancement factors for all log wood stoves as well as the LWB were comparable, with an average value around 10.

The variability in the EF_{ROS} in primary and aged OA for a single device was much higher than the variability between emission factors from different devices. A part of this variability within each device could be ascribed to the combustion phase, with higher emission factors for the starting and burn out phases compared to the flaming phase. This was especially true for the aged emissions from the PS, LWS2 and LWS3. Despite this, EF_{ROS} from the PB and MGB were on average one order of magnitude lower than those from the PS, LWB and LWS1-4. This indicates that applying automatic combustion devices operated at optimum conditions, to achieve near-complete combustion, is most effective to minimize ROS emissions. Although the EF_{ROS} showed somewhat different trends between devices with varying λ, a clear increase of EF_{ROS} in the aged aerosol can be observed from optimal to high lambda values; this emphasizing the important influence of the combustion conditions on EF_{ROS}. For the PB, the EF_{ROS} under λ^{opt} (λ = 1.6) did not statistically differ from that under λ^{-} ($\lambda \approx$ 1.3) conditions for both primary and secondary emissions (Mann-Whitney, *p*-value = 0.43 and 0.20, respectively). When comparing the EF_{ROS} under λ^{opt} and λ^{-} conditions with λ^{++} ($2.7 < \lambda < 3.4$) condition, primary EF_{ROS} under λ^{opt} and λ^{-} conditions were on average 7 and 3 times lower than that obtained under λ^{++} condition, respectively (Mann-Whitney, *p*-value < 0.005 for both cases). Aged EF_{ROS} under λ^{opt} and λ^{-} conditions were on average 8 and 5.5 times lower than obtained under λ^{++} condition, respectively (Mann-Whitney, *p*-value = 0.02 for both cases). In the MGB all the burns occurred at $2.0 < \lambda < 2.2$, leading to EF_{ROS} in line with those from the PB between λ^{opt} (λ = 1.6) and λ^{++} (where λ ranged from 2.7-3.4). The combustion in all stoves (PS, LWS1-4) exhibited higher λ ($\lambda > 2.2$) due to a less controlled air supply leading to a lower combustion temperature and increased products of incomplete combustion (less efficient combustion). In this range of oxygen excess, all aged EF_{ROS} were high but without any systematic trend with λ, suggesting that also other parameters influence ROS emissions. We further revealed that this variability was related to the bulk OA emissions, implying that this variation is inherent to the combustion conditions.

Nonetheless, the ROS content still varied by a factor of 2.6 on average for the same OA emission factor (EF_{OA}). We used a regression model on the data of SC and PAM chamber aging experiments to identify the different parameters that control the ROS secondary formation and content in OA upon aging. This regression model showed that the ROS contents in SOA (represented as $f_{ROS\text{-}SOA}$) depended significantly on all the aging parameters investigated, including the fractions of *m/z* 44 and *m/z* 43 in SOA, $f_{44\text{-}SOA}$ and $f_{43\text{-}SOA}$, respectively, the OH exposure and the organic aerosol mass concentration. The greatest share of explained variability in $f_{ROS\text{-}SOA}$ was attributed to $f_{44\text{-}SOA,}$ which indicates that the more oxygenated compounds are preferentially ROS active compared to others. The OH exposure was the second most important parameter controlling the aerosol ROS content under our condition where the anti-correlation between OH exposure and $f_{ROS\text{-}SOA}$ indicated that initially formed ROS are prone to further reactions. The organic mass and $f_{43\text{-}SOA}$ exhibited a low, but statistically significant effect on $f_{ROS\text{-}SOA}$. In summary, the ROS content seems to increase with the SOA oxidation state, which increases with OH exposure and decreases with the additional partitioning of semi-volatile components with lower ROS content at higher OA concentrations, while further aging seems to result in a decay of ROS.

The comparison and evolution of ROS with different combustion and aging conditions in this study might be used for a speedy assessment of potential health risks of wood combustion emissions from different combustion and aging conditions.

Acknowledgements

This study was financially supported by the Swiss National Science Foundation (NRP 70 "Energy Turnaround"), the European Union's Horizon 2020 research and innovation programme through the EUROCHAMP-2020 Infrastructure Activity under grant agreement No 730997, the Swiss National Science Foundation starting grant BSSGI0_155846, and the China Scholarship Council (CSC).

References

Adam, M., Schikowski, T., Carsin, A. E., Cai, Y., Jacquemin, B., Sanchez, M., Vierkötter, A., Marcon, A., Keidel, D., Sugiri, D., Al Kanani, Z., Nadif, R., Siroux, V., Hardy, R., Kuh, D., Rochat, T., Bridevaux, P.-O., Eeftens, M., Tsai, M.-Y., Villani, S., Phuleria, H. C., Birk, M., Cyrys, J., Cirach, M., de Nazelle, A., Nieuwenhuijsen, M. J., Forsberg, B., de Hoogh, K., Declerq, C., Bono, R., Piccioni, P., Quass, U., Heinrich, J., Jarvis, D., Pin, I., Beelen, R., Hoek, G., Brunekreef, B., Schindler, C., Sunyer, J., Krämer, U., Kauffmann, F., Hansell, A. L., Künzli, N., and Probst-Hensch, N.: Adult lung function and long-term air pollution exposure. ESCAPE: a multicentre cohort study and meta-analysis, Eur. Respir. J., 45, 38-50, https://doi.org/10.1183/09031936.00130014, 2015.

Andreae, M. O., and Merlet, P.: Emission of trace gases and aerosols from biomass burning, Global Biogeochem. Cycles, 15, 955-966, https://doi.org/10.1029/2000GB001382, 2001.

Barmet, P., Dommen, J., DeCarlo, P. F., Tritscher, T., Praplan, A. P., Platt, S. M., Prévôt, A. S. H., Donahue, N. M., and Baltensperger, U.: OH clock determination by proton transfer reaction mass spectrometry at an environmental chamber, Atmos. Meas. Tech., 5, 647-656, http://dx.doi.org/10.5194/amt-5-647-2012, 2012.

Beelen, R., Raaschou-Nielsen, O., Stafoggia, M., Andersen, Z. J., Weinmayr, G., Hoffmann, B., Wolf, K., Samoli, E., Fischer, P., Nieuwenhuijsen, M., Vineis, P., Xun, W. W., Katsouyanni, K., Dimakopoulou, K., Oudin, A., Forsberg, B., Modig, L., Havulinna, A. S., Lanki, T., Turunen, A., Oftedal, B., Nystad, W., Nafstad, P., De Faire, U., Pedersen, N. L., Östenson, C.-G., Fratiglioni, L., Penell, J., Korek, M., Pershagen, G., Eriksen, K. T., Overvad, K., Ellermann, T., Eeftens, M., Peeters, P. H., Meliefste, K., Wang, M., Bueno-de-Mesquita, B., Sugiri, D., Krämer, U., Heinrich, J., de Hoogh, K., Key, T., Peters, A., Hampel, R., Concin, H., Nagel, G., Ineichen, A., Schaffner, E., Probst-Hensch, N., Künzli, N., Schindler, C., Schikowski, T., Adam, M., Phuleria, H., Vilier, A., Clavel-Chapelon, F., Declercq, C., Grioni, S., Krogh, V., Tsai, M.-Y., Ricceri, F., Sacerdote, C., Galassi, C., Migliore, E., Ranzi, A., Cesaroni, G., Badaloni, C., Forastiere, F., Tamayo, I., Amiano, P., Dorronsoro, M., Katsoulis, M., Trichopoulou, A., Brunekreef, B., and Hoek, G.: Effects of long-term exposure to air pollution on natural-cause mortality: an analysis of 22 European cohorts within the multicentre ESCAPE project, The Lancet, 383, 785-795, https://doi.org/10.1016/S0140-6736(13)62158-3, 2013.

Bølling, A. K., Totlandsdal, A. I., Sallsten, G., Braun, A., Westerholm, R., Bergvall, C., Boman, J., Dahlman, H. J., Sehlstedt, M., Cassee, F., Sandstrom, T., Schwarze, P. E., and Herseth, J. I.: Wood smoke particles from different combustion phases induce similar pro-inflammatory effects in a co-culture of monocyte and pneumocyte cell lines, Part. Fibre Toxicol., 9, 45-45, https://doi.org/10.1186/1743-8977-9-45, 2012.

Bologa, A., Paur, H.-R., and Woletz, K.: Development and study of an electrostatic precipitator for small scale wood combustion, Environ. Sci. & Technol., 5, 168-173, http://www.isesp.org/ICESP%20XII%20PAPERS/pdfs/10_wed_m /043_Bologa.pdf, 2011.

Boman, B. C., Forsberg, A. B., and Järvholm, B. G.: Adverse health effects from ambient air pollution in relation to residential wood combustion in modern society, Scandinavian Journal of Work, Environ. & Health, 251-260, https://doi.org/10.5271/sjweh.729, 2003.

Bruns, E. A., El Haddad, I., Keller, A., Klein, F., Kumar, N. K., Pieber, S. M., Corbin, J. C., Slowik, J. G., Brune, W. H., Baltensperger, U., and Prévôt, A. S. H.: Inter-comparison of laboratory smog chamber and flow reactor systems on organic aerosol yield and composition, Atmos. Meas. Tech., 8, 2315-2332, https://doi.org/ 10.5194/ amt-8-2315 -2015, 2015.

Bruns, E. A., El Haddad, I., Slowik, J. G., Kilic, D., Klein, F., Baltensperger, U., and Prévôt, A. S. H.: Identification of significant precursor gases of secondary organic aerosols from residential wood combustion, Sci. Rep., 6, 27881, https://doi.org/10.1038/srep27881, 2016.

Bruns, E. A., Slowik, J. G., El Haddad, I., Kilic, D., Klein, F., Dommen, J., Temime-Roussel, B., Marchand, N., Baltensperger, U., and Prévôt, A. S. H.: Characterization of gas-phase organics using proton transfer reaction time-of-flight mass spectrometry: fresh and aged residential wood combustion emissions, Atmos. Chem. Phys., 17, 705-720, https://doi.org/10.5194/acp-17-705-2017, 2017.

EPBE: Impact of Residential Wood Stove Replacement on Air Emissions in Canada, in, Environmental Protection Branch Environment Canada, Montréal, 2005.

Ciarelli, G., Aksoyoglu, S., El Haddad, I., Bruns, E. A., Crippa, M., Poulain, L., Äijälä, M., Carbone, S., Freney, E., O'Dowd, C., Baltensperger, U., and Prévôt, A. S. H.: Modelling winter organic aerosol at the European scale with CAMx: evaluation and source apportionment with a VBS parameterization based on novel wood burning smog chamber experiments, Atmos. Chem. Phys., 17, 7653-7669, http://dx.doi.org/10.5194/acp-17-7653 -2017, 2017.

DeCarlo, P. F., Kimmel, J. R., Trimborn, A., Northway, M. J., Jayne, J. T., Aiken, A. C., Gonin, M., Fuhrer, K., Horvath, T., Docherty, K. S., Worsnop, D. R., and Jimenez, J. L.: Field-Deployable, High-Resolution, Time-of-Flight Aerosol Mass Spectrometer, Anal. Chem., 78, 8281-8289, https://doi.org/10.1021/ac061249n, 2006.

Dockery , D. W., Pope , C. A., Xu , X., Spengler , J. D., Ware , J. H., Fay , M. E., Ferris , B. G. J., and Speizer , F. E.: An Association between Air Pollution and Mortality in Six U.S. Cities, N. Engl. J. Med., 329, 1753-1759, https://doi.org/10.1056/nejm 199312093292401, 1993.

Drinovec, L., Močnik, G., Zotter, P., Prévôt, A. S. H., Ruckstuhl, C., Coz, E., Rupakheti, M., Sciare, J., Müller, T., Wiedensohler, A., and Hansen, A. D. A.: The "dual-spot" Aethalometer: an improved measurement of aerosol black carbon with real-time loading compensation, Atmos. Meas. Tech., 8, 1965-1979, http://dx.doi.org/10.5194/amt-8-1965-2015, 2015.

EEA: European Union emission inventory report 1990-2011 under the UNECE Convention on Long-range Transboundary Air Pollution (LRTAP), in: EEA Technical report, EEA (European Environment Agency), Copenhagen, 2013a.

EEA: European Union emission inventory report 1990-2011 under the UNECE Convention on Long-range Transboundary Air Pollution (LRTAP), in: Technical report, European Environment Agency (EEA), Copenhagen, 2013b.

Fitzpatrick, E. M., Ross, A. B., Bates, J., Andrews, G., Jones, J. M., Phylaktou, H., Pourkashanian, M., and Williams, A.: Emission of Oxygenated Species from the Combustion of Pine Wood and its Relation to Soot Formation, Process Saf. Environmental Protection, 85, 430-440, http://dx.doi.org/10.1205/psep07020, 2007.

Fu, P. P., Xia, Q., Sun, X., and Yu, H.: Phototoxicity and Environmental Transformation of Polycyclic Aromatic Hydrocarbons (PAHs)—Light-Induced Reactive Oxygen Species, Lipid Peroxidation, and DNA Damage, J. Environ. Sci. Health, Part C, 30, 1-41, http://dx.doi.org/10.1080/10590501.2012.653887, 2012.

Fuller, G. W., Tremper, A. H., Baker, T. D., Yttri, K. E., and Butterfield, D.: Contribution of wood burning to PM10 in London, Atmos. Environ., 87, 87-94, http://dx.doi.org/10.1016/j.atmosenv.2013.12.037, 2014a.

Fuller, S. J., Wragg, F. P. H., Nutter, J., and Kalberer, M.: Comparison of on-line and off-line methods to quantify reactive oxygen species (ROS) in atmospheric aerosols, Atmos. Environ., 92, 97-103, http://dx.doi.org/10.1016/j.atmosenv.2014.04.006, 2014b.

Fullerton D. G., Semple A. S., S., Kalambo F., Malamba R., White S., Jack S., Calverley P. M., Gordon S. B.: Wood smoke exposure, poverty and impaired lung function in Malawian adults, Int. J. Tuberc. Lung Dis., 15, 391-398, http://www.ingentaconnect.com/.../ijtld, 2011.

He, T., Yang, Z., Liu, T., Shen, Y., Fu, X., Qian, X., Zhang, Y., Wang, Y., Xu, Z., Zhu, S., Mao, C., Xu, G., and Tang, J.: Ambient air pollution and years of life lost in Ningbo, China, 6, 22485, http://dx.doi.org/10.1038/srep22485, 2016.

Heringa, M. F., DeCarlo, P. F., Chirico, R., Tritscher, T., Dommen, J., Weingartner, E., Richter, R., Wehrle, G., Prévôt, A. S. H., and Baltensperger, U.: Investigations of primary and secondary particulate matter of different wood combustion appliances with a high-resolution time-of-flight aerosol mass spectrometer, Atmos. Chem. Phys., 11, 5945-5957, http://dx.doi.org/10.5194/acp-11-5945-2011, 2011.

Huang, W., Zhang, Y., Zhang, Y., Fang, D., and Schauer, J. J.: Optimization of the Measurement of Particle-Bound Reactive Oxygen Species with 2′,7′-dichlorofluorescin (DCFH), Water Air Soil Pollut., 227, http://dx.doi.org/10.1007/s11270-016-2860-9, 2016.

Hwang, B.-F., Chen, Y.-H., Lin, Y.-T., Wu, X.-T., and Leo Lee, Y.: Relationship between exposure to fine particulates and ozone and reduced lung function in children, Environ. Res., 137, 382-390, http://dx.doi.org/10.1016/j.envres.2015.01.009, 2015.

Liu, J. C., Wilson A., Mickley L. J., Dominici F., Ebisu K., Wang Y., Sulprizio M. P., Peng R. D., Yue X., Son J. Y., Anderson G. B., and Bell, M. L.: Wildfire-specific Fine Particulate Matter and Risk of Hospital Admissions in Urban and Rural Counties, Epidemiology, 28, 77-85, http://dx.doi.org/10.1097/EDE.0000000000000556, 2017.

Johansson, L. S., Leckner, B., Gustavsson, L., Cooper, D., Tullin, C., and Potter, A.: Emission characteristics of modern and old-type residential boilers fired with wood logs and wood pellets, Atmos. Environ., 38, 4183-4195, http://dx.doi.org/10.1016/j.atm osenv.2004.04.020, 2004.

Johnston, F. H., Henderson, S. B., Chen, Y., Randerson, J. T., Marlier, M., Defries, R. S., Kinney, P., Bowman, D. M., and Brauer, M.: Estimated global mortality attributable to smoke from landscape fires, Environ. Health Perspect., 120, 695-701, http://dx.doi.org/ 10.1289/ehp.1104422, 2012.

Kang, E., Root, M. J., Toohey, D. W., and Brune, W. H.: Introducing the concept of Potential Aerosol Mass (PAM), Atmos. Chem. Phys., 7, 5727-5744, http://dx.doi.org/10.5194/acp -7 -5727-2007, 2007.

Kelly, F. J., and Fussell, J. C.: Size, source and chemical composition as determinants of toxicity attributable to ambient particulate matter, Atmos. Environ., 60, 504-526, http://dx.doi.org/10.1016/j.atmosenv.2012.06.039, 2012.

King, L. E., and Weber, R. J.: Development and testing of an online method to measure ambient fine particulate reactive oxygen species (ROS) based on the 2',7'-dichlorofluorescin (DCFH) assay, Atmos. Meas. Tech., 6, 1647-1658, http://dx.doi.org/10.5194/amt-6-1647-2013, 2013.

Krapf, M., Kunzi, L., Allenbach, S., Bruns, E. A., Gavarini, I., El-Haddad, I., Slowik, J. G., Prevot, A. S. H., Drinovec, L., Mocnik, G., Dumbgen, L., Salathe, M., Baumlin, N., Sioutas, C., Baltensperger, U., Dommen, J., and Geiser, M.: Wood combustion particles induce adverse effects to normal and diseased airway epithelia, Environ. Sci.-Proc. Imp., 19, 538-548, http://dx.doi.org/10.1039/C6EM00586A, 2017.

Lee, Y. L., Wang, W.-H., Lu, C.-W., Lin, Y.-H., and Hwang, B.-F.: Effects of ambient air pollution on pulmonary function among schoolchildren, Int. J. Hyg. and Environ. Health, 214, 369-375, http://dx.doi.org/10.1016/j.ijheh.2011.05.004, 2011.

Lobo, V., Patil, A., Phatak, A., and Chandra, N.: Free radicals, antioxidants and functional foods: Impact on human health, Pharmacogn. Rev., 4, 118-126, http://dx.doi.org/10.4103/0973-7847.70902, 2010.

Marabini, L., Ozgen, S., Turacchi, S., Aminti, S., Arnaboldi, F., Lonati, G., Fermo, P., Corbella, L., Valli, G., Bernardoni, V., Dell'Acqua, M., Vecchi, R., Becagli, S., Caruso, D., Corrado, G. L., and Marinovich, M.: Ultrafine particles (UFPs) from domestic wood stoves: genotoxicity in human lung carcinoma A549 cells, Mutat. Res., 820, 39-46, http://dx.doi.org/10.1016/j.mrgentox.2017.06.001, 2017.

Miljevic, B., Heringa, M. F., Keller, A., Meyer, N. K., Good, J., Lauber, A., DeCarlo, P. F., Fairfull-Smith, K. E., Nussbaumer, T., Burtscher, H., Prevot, A. S. H., Baltensperger, U., Bottle, S. E., and Ristovski, Z. D.: Oxidative Potential of Logwood and Pellet Burning Particles Assessed by a Novel Profluorescent Nitroxide Probe, Environ. Sci. Technol., 44, 6601-6607, http://dx.doi.org/10.1021/es100963y, 2010.

Muala, A., Rankin, G., Sehlstedt, M., Unosson, J., Bosson, J. A., Behndig, A., Pourazar, J., Nyström, R., Pettersson, E., Bergvall, C., Westerholm, R., Jalava, P. I., Happo, M. S., Uski, O., Hirvonen, M.-R., Kelly, F. J., Mudway, I. S., Blomberg, A., Boman, C., and Sandström, T.: Acute exposure to wood smoke from incomplete combustion - indications of cytotoxicity, Part. Fibre Toxicol., 12, 33, http://dx.doi.org/10.1186/s12989-015-0111-7, 2015.

Nussbaumer T. and Kaltschmitt M.: 8.1 Begriffsdefinitionen, in M. Kaltschmitt and H. Hartmann (Eds.), Energie aus Biomasse: Springer, Berlin, Heidelberg, 239–247, 2000.

Nussbaumer, T.: Combustion and Co-combustion of Biomass: Fundamentals, Technologies, and Primary Measures for Emission Reduction, Energy Fuels, 17, 1510-1521, http://dx.doi.org/10.1021/ef030031q, 2003.

Nussbaumer, T., and Lauber, A.: Formation mechanisms and physical properties of particles from wood combustion for design and operation of electrostatic precipitators, 18th European Biomass Conference and Exhibition, Lyon, ETA-Florence, 3–7 May 2010, 2010.

Paulsen, D., Dommen, J., Kalberer, M., Prévôt, A. S. H., Richter, R., Sax, M., Steinbacher, M., Weingartner, E., and Baltensperger, U.: Secondary Organic Aerosol Formation by Irradiation of 1,3,5-Trimethylbenzene−NOx−H2O in a New Reaction Chamber for Atmospheric Chemistry and Physics, Environ. Sci. Technol., 39, 2668-2678, http://dx.doi.org/10.1021/es0489137, 2005.

Pfaffenberger, L., Barmet, P., Slowik, J. G., Praplan, A. P., Dommen, J., Prévôt, A. S. H., and Baltensperger, U.: The link between organic aerosol mass loading and degree of oxygenation: an α-pinene photooxidation study, Atmos. Chem. Phys., 13, 6493-6506, http://dx.doi.org/10.5194/acp-13-6493-2013, 2013.

Platt, S. M., El Haddad, I., Zardini, A. A., Clairotte, M., Astorga, C., Wolf, R., Slowik, J. G., Temime-Roussel, B., Marchand, N., Ježek, I., Drinovec, L., Močnik, G., Möhler, O., Richter, R., Barmet, P., Bianchi, F., Baltensperger, U., and Prévôt, A. S. H.: Secondary organic aerosol formation from gasoline vehicle emissions in a new mobile environmental reaction chamber, Atmos. Chem. Phys., 13, 9141-9158, http://dx.doi.org/10.5194/acp-13-9141-2013, 2013.

Platt, S. M., Haddad, I. E., Pieber, S. M., Huang, R. J., Zardini, A. A., Clairotte, M., Suarez-Bertoa, R., Barmet, P., Pfaffenberger, L., Wolf, R., Slowik, J. G., Fuller, S. J., Kalberer, M., Chirico, R., Dommen, J., Astorga, C., Zimmermann, R., Marchand, N., Hellebust, S., Temime-Roussel, B., Baltensperger, U., and Prévôt, A. S. H.: Two-stroke scooters are a dominant source of air pollution in many cities, Nat. Commun., 5, 3749, http://dx.doi.org/10.1038/ncomms4749, 2014.

Pope, I. C., Burnett, R. T., Thun, M. J., and et al.: Lung cancer, cardiopulmonary mortality, and long-term exposure to fine particulate air pollution, JAMA, 287, 1132-1141, http://dx.doi.org/10.1001/jama.287.9.1132, 2002.

Schmidl, C., Luisser, M., Padouvas, E., Lasselsberger, L., Rzaca, M., Ramirez-Santa Cruz, C., Handler, M., Peng, G., Bauer, H., and Puxbaum, H.: Particulate and gaseous emissions from manually and automatically fired small scale combustion systems, Atmos. Environ., 45, 7443-7454, http://dx.doi.org/10.1016/j.atmosenv.2011.05.006, 2011.

Tapanainen, M., Jalava, P. I., Mäki-Paakkanen, J., Hakulinen, P., Lamberg, H., Ruusunen, J., Tissari, J., Jokiniemi, J., and Hirvonen, M.-R.: Efficiency of log wood combustion affects the toxicological and chemical properties of emission particles, Inhal. Toxicol., 24, 343-355, http://dx.doi.org/10.3109/08958378.2012.671858, 2012.

Tapanainen, M., Jalava, P. I., Mäki-Paakkanen, J., Hakulinen, P., Lamberg, H., Ruusunen, J., Tissari, J., Jokiniemi, J., and Hirvonen, M.-R.: Efficiency of log wood combustion affects the toxicological and chemical properties of emission particles, Inhal. Toxicol., 24, 343-355, http://dx.doi.org/10.3109/08958378.2012.671858, 2012.

U.S. Environmental Protection Administration (USEPA): National emission trends (NET) database, Emission Factor and Inventory Group, Office of Air Quality Planning and Standards, in, Research Triangle Park, N.C., 2000.

Urs Baltensperger, Josef Dommen, M. Rami Alfarra, Jonathan Duplissy, Kathrin Gaeggeler, Axel Metzger, Maria Cristina Facchini, Stefano Decesari, Emanuela Finessi, Christopher Reinnig, Mathias Schott, Jörg Warnke, Thorsten Hoffmann, Barbara Klatzer, Hans Puxbaum, Marianne Geiser, Melanie Savi, Doris Lang, Markus Kalberer, and Geise, a. T.: Combined Determination of the Chemical Composition and of Health Effects of Secondary Organic Aerosols: The POLYSOA Project, J, Aerosol Med. Pul. Drug Deliv., 21, 145-154, http://dx.doi.org/10.1089/jamp.2007.0655, 2008.

Venkatachari, P., and Hopke, P. K.: Development and Laboratory Testing of an Automated Monitor for the Measurement of Atmospheric Particle-Bound Reactive Oxygen Species (ROS), Aerosol Science and Technology, 42, 629-635, http://dx.doi.org/10.1080/02786820802227345, 2008.

Verma, V., Fang, T., Xu, L., Peltier, R. E., Russell, A. G., Ng, N. L., and Weber, R. J.: Organic Aerosols Associated with the Generation of Reactive Oxygen Species (ROS) by Water-Soluble $PM_{2.5}$, Environ. Sci. Technol., 49, 4646-4656, http://dx.doi.org/10.1021/es505577w, 2015.

Wang, Y., Hopke, P.K., Sun, L., Chalupa, D.C., and Utell, M.J.,: Laboratory and field testing of an automated atmospheric particle-bound reactive oxygen species sampling-analysis system. J. Toxicol., 419-476, http://dx.doi.org/10.1155/2011/419476, 2011.

Wang, S., Sheng, Y., Feng, M., Leszczynski, J., Wang, L., Tachikawa, H., and Yu, H.: Light-Induced Cytotoxicity of 16 Polycyclic Aromatic Hydrocarbons on the US EPA Priority Pollutant List in Human Skin HaCaT Keratinocytes: Relationship Between Phototoxicity and Excited State Properties, Environ. toxicol., 22, 318-327, http://dx.doi.org/10.1002/tox.20241, 2007.

Ward, D. E., and Radke, L. F.: Emission measurements from vegetation fires: A comparative evalution of methods and results, in: Fire in the Environment: The Ecological, atmospheric and Climatic Importance of Vegetation Fires, edited by: Crutzen, P. J., and Goldammer, J. G., John Wilry, Chichester UK, 53-56, 1993.

Yap, S. G. P.: The Potential Impact of Residential Wood Burning Regulations in a California Region: Concurrent Wintertime Reductions in Ambient Pollution and Cardiovascular Mortality, ISEE 20th Annual Conference, Pasadena, California, USA, 2008.

Zhang, X., Hecobian, A., Zheng, M., Frank, N. H., and Weber, R. J.: Biomass burning impact on $PM_{2.5}$ over the southeastern US during 2007: integrating chemically speciated FRM filter measurements, MODIS fire counts and PMF analysis, Atmos. Chem. Phys., 10, 6839-6853, http://dx.doi.org/10.5194/acp-10-6839-2010, 2010.

Zhou, J., Bruns, E. A., Zotter, P., Stefenelli, G., Prévôt, A. S. H., Baltensperger, U., Ei-Haddad, I., and Dommen, J.: Development, characterization and first deployment of an improved online reactive oxygen species analyzer, Atmos. Meas. Tech. Discuss., 2017, 1-27, http://dx.doi.org/10.5194/amt-2017-161, 2017.

Zhou, M., Diwu, Z., Panchuk-Voloshina, N., and Haugland, R. P.: A stable nonfluorescent derivative of resorufin for the fluorometric determination of trace hydrogen peroxide: applications in detecting the activity of phagocyte NADPH oxidase and other oxidases, Anal. biochem., 253, 162-168, http://dx.doi.org/10.1006/abio.1997.2391, 1997.